**HIGH POWER LASER**
SCIENCE AND ENGINEERING

RESEARCH ARTICLE

# A 5.32 mJ and 47.5 kW cavity-dumped $Pr^{3+}$:$LiYF_4$ pulsed laser at 639 nm

Wei Yuan[1,2,3], Shaoqiang Zheng[2,3], Zheng Zhang[2,3], Yongkang Yao[2,3], Huiying Xu[2,3], and Zhiping Cai [2,3]

[1] *Center for Modern Educational Technology, Guizhou Normal University, Guiyang, China*

[2] *School of Electronic Science and Engineering, Xiamen University, Xiamen, China*

[3] *Fujian Key Laboratory of Ultrafast Laser Technology and Applications, Xiamen University, Xiamen, China*

**Abstract**

In this work, we confirm a $Pr^{3+}$:$LiYF_4$ pulsed laser with high power and high energy at 639 nm based on the acousto-optic cavity dumping technique. The maximum average output power, narrowest pulse width, highest pulse energy and peak power of the pulsed laser at a repetition rate of 0.1 kHz are 532 mW, 112 ns, 5.32 mJ and 47.5 kW, respectively. A 639 nm pulsed laser with such high pulse energy and peak power has not been reported previously. Furthermore, we obtain a widely tunable range of repetition rates from 0.1 to 5000 kHz. The diffracted beam quality factors $M^2$ are 2.18 (in the $x$ direction) and 2.04 (in the $y$ direction). To the best of our knowledge, this is the first time that a cavity-dumped all-solid-state pulsed laser in the visible band has been reported. This work provides a promising method for obtaining high-performance pulsed lasers.

**Keywords:** 639 nm; cavity dumping technique; $Pr^{3+}$:$LiYF_4$; pulsed laser

## 1. Introduction

Visible lasers have important applications in biomedical, industrial processing, communications and military fields[1–5]. There have been numerous reports on continuous-wave (CW) visible lasers based on $Pr^{3+}$:$LiYF_4$ (Pr:YLF) crystals[6–9]. Compared to the green laser, orange laser and other bands, the laser at 639 nm has the highest emission cross-section of approximately $22.3 \times 10^{-20}$ cm²[10,11], which implies that the highest output power may be obtained at the wavelength of 639 nm on Pr:YLF. To the best of our knowledge, the highest output power of CW lasers reported at 639 nm is 8.14 W[12]. However, this output power is not sufficient for some specific applications, for example, metal cutting. Pulsed lasers are becoming a hot spot for research because of their potential of high power and high energy.

Several studies have been reported on 639 nm Pr:YLF pulsed lasers. The methods used in reports mainly include active *Q*-switching and passive *Q*-switching. In 2014, based on a Pr:YLF crystal, Kojou *et al.*[13] used an acousto-optic modulator (AOM) as a modulating switch to obtain 320 and 261 nm pulsed lasers by intracavity frequency doubling in the experiment. The pulse width, pulse energy and peak power of the 640 nm pulsed laser at a repetition rate of 7.7 kHz are obtained as 17 ns, 27 µJ and 1.57 kW, respectively. In 2020, Jin *et al.*[14] used the method of *Q*-switched pre-lasing in conjunction with a Fabry–Pérot etalon to obtain a single-longitudinal-mode 639 nm Pr:YLF pulsed laser directly. The pulse width, peak power and single-pulse energy at a repetition rate of 10 kHz are 81.1 ns, 48.5 W and 3.94 µJ, respectively. In 2022, under the pumping of a blue laser diode (LD), Yang *et al.*[15] obtained a Pr:YLF high-energy pulsed laser at 639 nm for the first time by electro-optic *Q*-switching. The highest pulse energy, peak power, pulse width and average power are 260 µJ, 1898 W, 137 ns and approximately 26 mW, respectively and the tunable range of repetition rate is from 100 to 500 Hz; the pulse energy and peak power have the highest values at that time. In 2024, under the pumping of a 24 W blue light pump source, Xue *et al.*[16] obtained a 639 nm Pr:YLF pulsed laser with watt-level average power for the first time,

---

Correspondence to: Z. Cai, School of Electronic Science and Engineering, Xiamen University, Xiamen 361005, China. Email: zpcai@xmu.edu.cn
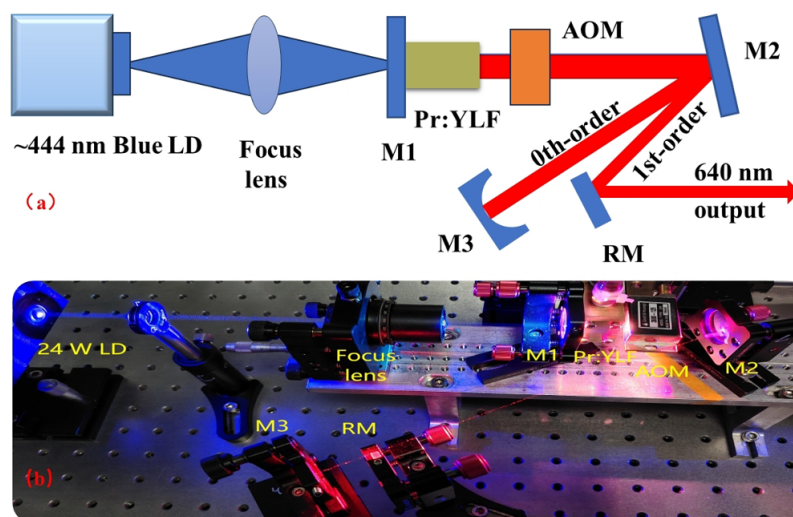
**Figure 1.** (a) Schematic diagram of the experimental setup. (b) Physical diagram of the experimental setup.

in which an AOM was used as the *Q*-switch. The pulse width, average output power, pulse energy and peak power are 40 ns, 1.136 W, 110 µJ and 2.796 kW, respectively. In 2021, Badtke *et al.*[17] presented passive *Q*-switching at 640 nm using $Co:MgAl_2O_4$ as a saturable absorber, with the narrowest pulse width of 8.5 ns at a repetition rate of 0.78 MHz. However, the average output power, pulse energy and peak power were not so good, corresponding to values of 1 W, 1.3 µJ and 140 W, respectively. From the works reported above, it is easy to see that the pulse energy and peak power of the 639 nm laser are still relatively low, the tunable range of the repetition rate is narrow and a stable 639 nm pulsed laser at high repetition rate has not been realized.

As far as we know, pulsed lasers based on the cavity dumping technique are mainly focused on the near-infrared band, for example, 1989.8 nm[18], 2013 nm[19] and 2012.6 nm[20]. The gain mediums are mainly thulium-doped yttrium aluminum perovskite (Tm:YAP), thulium-doped yttrium aluminum garnet (Tm:YAG), neodymium-doped gadolinium orthovanadate (Nd:GdVO$_4$), etc., while cavity-dumped pulsed lasers based on Pr:YLF crystals have not been reported to date.

In this work, we use an AOM as the modulating switch and a Pr:YLF crystal as the gain medium. The first-order diffracted laser separated from the AOM is reflected out of the resonant cavity as the output laser. We obtain a pulsed laser with a widely tunable repetition rate range from 0.1 to 5000 kHz, and the average output power, pulse width, pulse energy and peak power of the 639 nm pulsed laser are 532 mW, 112 ns, 5.32 mJ and 47.5 kW at a repetition rate of 0.1 kHz, respectively. An order-of-magnitude increase in pulse energy and peak power of the 639 nm pulsed laser is achieved. As a result, a 639 nm high-performance pulsed laser based on the acousto-optic cavity dumping technique is obtained.

## 2. Experimental setup

As shown in Figure 1, the coupled mirrors M1, M2 and M3 are used to form a V-shaped resonant cavity. A commercial 24 W blue LD is used as the pump source, which has a vertically polarized continuous light with a central wavelength of 444 nm. The pump light is focused into the crystal by the focusing of a 75 mm plano-convex focus lens, and the waist radius of the pump light is measured to be approximately 123 µm. M1 and M2 are plane mirrors with high transmittance at 444 nm; the transmittance values are 98.14% and 91.49%, respectively; they have high reflectivity for red light at 639 nm and the transmittance is almost 0. M3 is a concave mirror with a radius of curvature of 300 mm, which is highly reflective of red light at 639 nm (transmittance of ~0.39%). The transmittance curves of the three coupled mirrors are shown in Figure 2. The AOM (model 3080-125, Gooch & Housego) is used for the switching control of the laser at 639 nm, which has the tunable wavelength range of 450–850 nm, the active aperture of 2.5 mm (*L*) × 2.0 mm (*H*), the rise/fall time of 25 ns, the center frequency of 80 MHz and the radio frequency (RF) bandwidth of 25 MHz @ –9 dB return loss. Under the modulating of the AOM, the diffracted lasers of zeroth-order and first-order are generated. RM is a plane mirror with high reflectivity at 639 nm and high transmittance at 444 nm, which is used to reflect the first-order diffracted laser outside the resonant cavity. The gain medium used in the experiments is an *a*-cut Pr:YLF crystal with length of 14 mm, which has a doping concentration of 0.15% (atomic fraction), in which the size of the polished facets is 3 mm × 3 mm. The crystal is wrapped in indium foil, and placed inside a copper block, with its *π* direction parallel to the vertical direction, which is cooled by a water-cooling system set at 10°C. As a result, we successfully obtain a
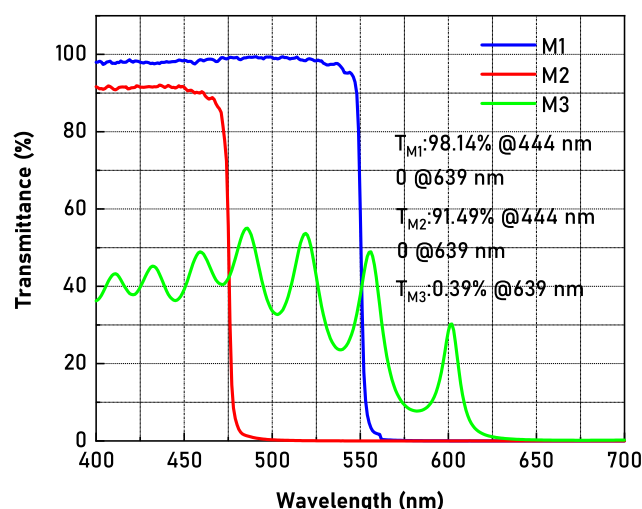
**Figure 2.** Optical transmittance properties of M1, M2 and M3.



**Figure 3.** Maximum average output power at different repetition rates (0.1, 600, 1000, 2000, 3000, 4000 and 5000 kHz). The inset shows the average output power versus absorbed pump power at repetition rates of 0.1 and 5000 kHz.

cavity-dumped pulsed laser by optimizing the resonant cavity and adjusting the angle of the AOM.

We calculate the waist radius of the laser in the crystal and the laser size (close to the crystal) at the end face of the AOM, and they are approximately 41 and 42.7 μm, respectively.

## 3. Results and discussion

In the experiment, the power absorption efficiency of the Pr:YLF crystal is about 43%. We find that the output power is saturated with the increase of pump power, and the maximum absorbed pump power of the crystal is about 7.3 W. In order to protect the crystal from damage, we do not continue to increase the pump power. In our opinion, the short length of the crystal and the shift in the central wavelength of the pump source at high power are the main reasons for the unsatisfactory absorption efficiency.

As shown in Figure 3, under the pumping of maximum absorbed pump power, we measure the average output power of the first-order diffracted laser at different repetition rates. At a repetition rate of 0.1 kHz, we obtain a pulsed laser with maximum average output power of 532 mW, and the maximum average output power is 453 mW at a repetition rate of 5000 kHz. It can be seen that the average output power shows an overall decreasing trend. In our view, this is related to the evolution of population inversion density and photon density in the cavity. The lifetime of the upper energy level ($^3$P$_0$) at the wavelength of 639 nm based on the Pr:YLF crystal is approximately 50 μs[21–23]. When the pulse interval of the pulsed laser is less than 50 μs (repetition rate > 20 kHz), this will result in insufficient accumulation of the inverted population in the upper energy level. As the repetition rate increases, the population inversion density accumulated in the upper
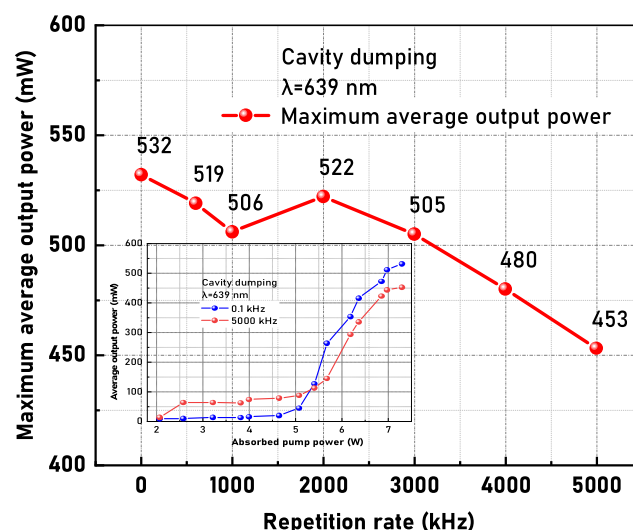
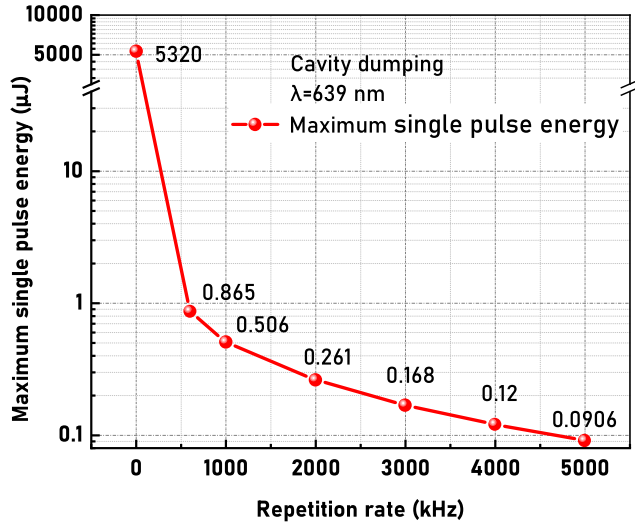energy level decreases, and the average output power decreases.

The inset in Figure 3 shows the absorbed pump power versus the average output power at repetition rates of 0.1 and 5000 kHz. It is not difficult to see that as the absorbed pump power increases, the average output power shows an increasing trend. When the absorbed pump power is greater than 7 W, the average output power shows significant saturation.

When coating the film for M3, even though we set the transmittance to zero at the wavelength of 639 nm, the ideal fully reflective mirror is difficult to obtain. As we present in Figure 2, the real transmittance of M3 at 639 nm is 0.39%. According to the principle of obtaining pulsed lasers by the cavity dumping technique, this will reduce the output power of first-order diffracted lasers. We believe that replacing M3 with a fully reflective mirror at 639 nm will improve the output power of first-order diffracted light.

At the maximum absorbed pump power, we record the narrowest pulse widths at different repetition rates, as shown in Figure 4. The narrowest pulse widths at repetition rates of 0.1 and 5000 kHz are 112 and 77.5 ns, respectively. As the repetition rate increases, the narrowest pulse width slightly decreases. We believe that the probable cause of the decreasing trend in pulse width is due to the non-standard output of square wave pulses from the signal source. The pulse width of the cavity-dumped pulsed laser is mainly related to the length of the resonant cavity and the switching speed of the AOM. The real length of the resonant cavity is approximately 270 mm, and the rising or falling edge time of the AOM is 25 ns. We believe that shortening the length of the resonant cavity and replacing the AOM with shorter rising or falling edge time are beneficial for obtaining
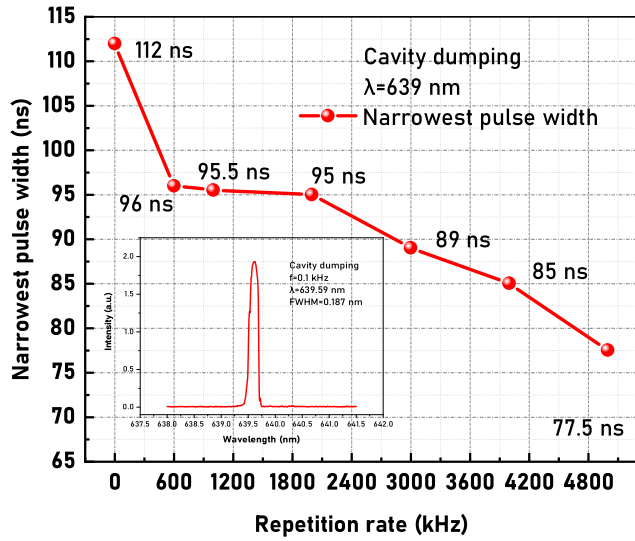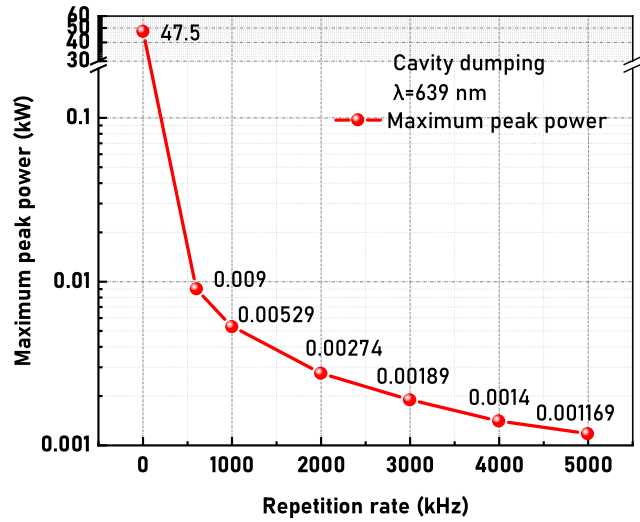
**Figure 4.** Narrowest pulse width at different repetition rates (0.1, 600, 1000, 2000, 3000, 4000 and 5000 kHz). The inset shows the spectrum at 0.1 kHz.
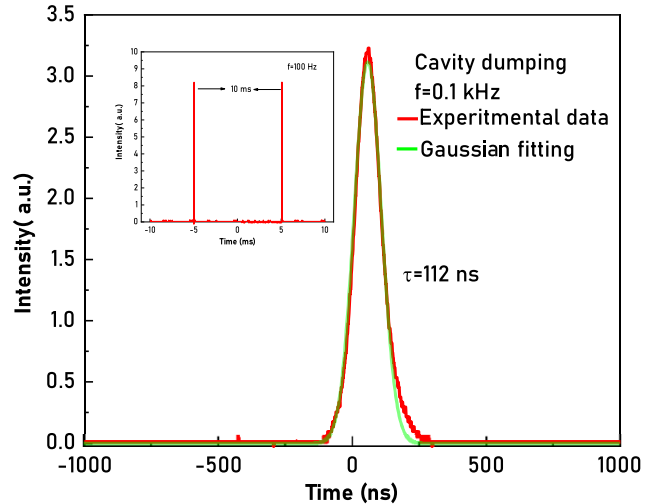


**Figure 6.** Maximum peak power at different repetition rates (0.1, 600, 1000, 2000, 3000, 4000 and 5000 kHz).



**Figure 5.** Maximum single-pulse energy at different repetition rates (0.1, 600, 1000, 2000, 3000, 4000 and 5000 kHz).



**Figure 7.** Single-pulse and typical pulse train (inset) at the repetition rate of 0.1 kHz.

a narrower pulse width of the pulsed laser. The inset shows the spectrum at a repetition rate of 0.1 kHz, with a central wavelength of 639.59 nm and a full width at half maximum (FWHM) of 0.187 nm. We measure the spectrum using an Advantest Q8341 instrument.

According to the equations for pulse energy and peak power, $E = P/f$ and $P_{peak} = E/\tau$[24], where $E$, $P$, $f$, $P_{peak}$ and $\tau$ are the single-pulse energy, average output power, repetition rate, peak power and pulse width, respectively. Figure 5 shows the curve of maximum pulse energy at different repetition rates. As we can see, the maximum single-pulse energy of 5320 μJ is at a repetition rate of 0.1 kHz, which, to the best of our knowledge, is the maximum single-pulse energy at 639 nm reported so far. As the repetition rate increases,

the maximum single-pulse energy decreases rapidly. In our opinion, the increase in repetition rate leads to an increase in the number of pulses per unit time in the cavity dumping operation, while the average output power does not increase, which results in a smaller single-pulse energy. As shown in Figure 6, we achieve the maximum peak power of 47.5 kW at the repetition rate of 0.1 kHz. As far as we know, this is the first time that a 639 nm pulsed laser with such high peak power has been obtained. The pulse energy and peak power of the pulsed laser at 639 nm have been greatly improved in this work.

Figure 7 demonstrates the spectral characteristics of the 639 nm pulsed laser at a repetition rate of 0.1 kHz. We can see that the spectrum with the pulse width of 112 ns overlaps well with the curve by Gaussian fitting, which proves the formation of a Gaussian-like laser. The inset shows the pulse
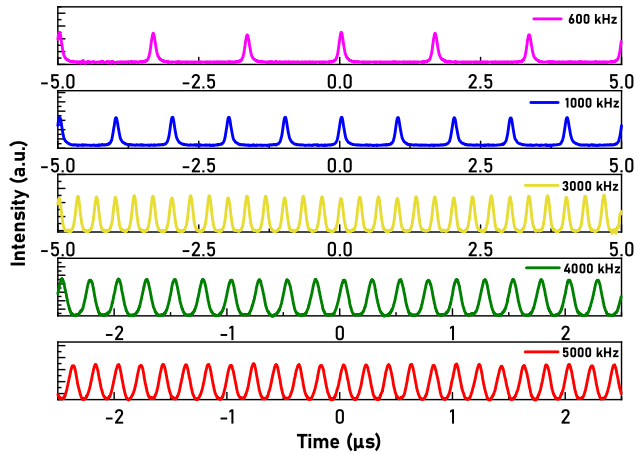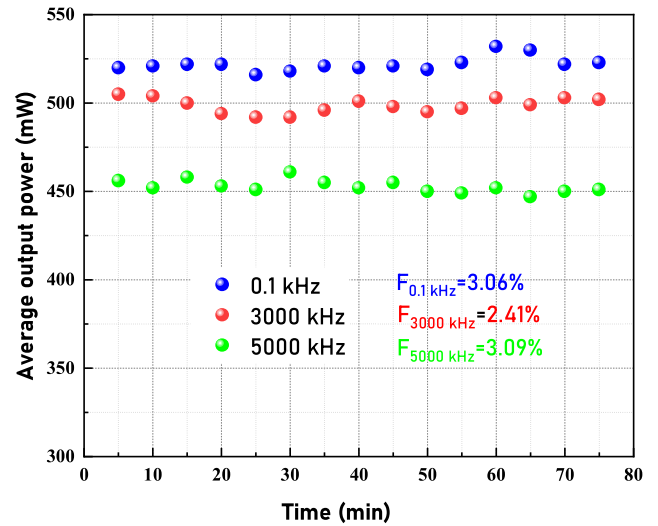
**Figure 8.** Typical pulse trains at different repetition rates (600, 1000, 3000, 4000 and 5000 kHz).



**Figure 9.** Stability of maximum average output power at different repetition rates (0.1, 3000 and 5000 kHz).

train recorded by the oscilloscope; the fluctuation of the pulse train is approximately 1%.

Figure 8 shows the pulse trains of the 639 nm pulsed laser at different repetition rates of 600, 1000, 2000, 3000, 4000 and 5000 kHz. We can see that cavity-dumped lasers have advantages with a wide range of tunable repetition rates (from 0.1 to 5000 kHz in this work) over *Q*-switched pulsed lasers, wherein the highest tunable repetition rates of *Q*-switched pulsed lasers are generally at tens or hundreds of kHz[16,25,26]. It is not difficult to see that within the range of tunable repetition rates, the pulse trains of the pulsed laser are very stable. What is more, this work provides a very promising method for obtaining pulsed lasers with a high repetition rate. In this experiment, in order to ensure the time conditions of accumulation of the inverted population and photon oscillation in the cavity at different repetition rates, we adjust slightly the duty cycle of the pulse signal input by the signal generator.

Under the maximum absorbed pump power, the stabilities of maximum average output power are recorded at different repetition rates. As shown in Figure 9, the power fluctuations at different repetition rates of 0.1, 3000 and 5000 kHz are 3.06%, 2.41% and 3.09%, respectively. We believe that the stability of the pump source is the key to the stability of maximum average output power. Based on our experimental experience, the unstable diffraction of the AOM is also one of the factors affecting the stability of the maximum average output power. In addition, the thermal lensing effect of the crystal can lead to instability of the output power.

Figure 10 demonstrates the laser beam quality of the cavity-dumped pulsed laser. At the maximum output power, the beam quality factors $M^2$ are 2.18 (in the *x* direction) and 2.04 (in the *y* direction) at the repetition rate of 0.1 kHz. The inset shows the beam profile captured by a charge-coupled device (CCD) camera; this reconfirms that the pulsed laser is a Gaussian-like laser.
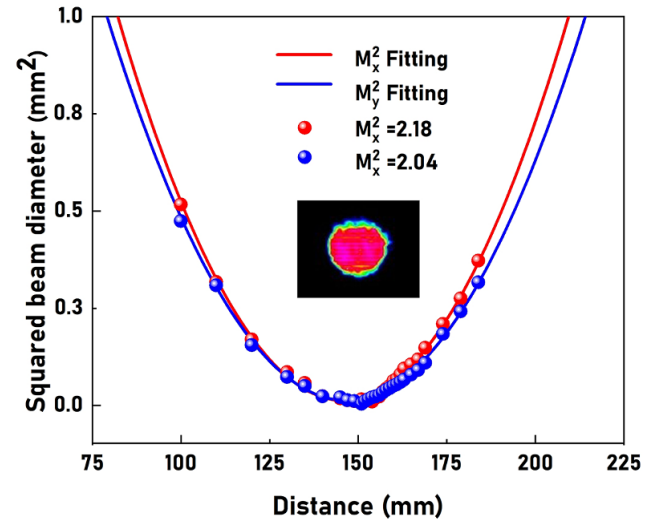


**Figure 10.** Beam quality $M^2$ factors of the cavity-dumped laser at 639 nm and beam profile captured by the CCD camera.

During the experiment, the thermal lensing effect of the crystal inevitably affects the beam quality. We think that lowering the temperature of the cooling system would improve the beam quality of the pulsed laser. However, since the temperature of the laboratory could not be lowered any further, this difference of temperature with the copper block and air in the laboratory would lead to the condensation of water droplets on the surface of the copper block, which is a serious threat to the safety of the Pr:YLF crystal. Therefore, we maintain the temperature of the cooling system at 10°C. In addition, the stability of the pump source also affects the beam quality of the pulsed laser.

In order to visually compare the performance of 639 nm pulsed lasers, we list several representative reports in Table 1.

**Table 1.** Performance comparison of pulsed lasers at 639 nm[a].

| Operation regime | Average power (mW) | Pulse width (ns) | Pulse energy (μJ) | Peak power (kW) | Repetition rate (kHz) | Reference |
|---|---|---|---|---|---|---|
| AO switching | | 17 | 27 | 1.57 | 7.7 | [13] |
| AO switching | | 81.1 | 3.94 | 0.0485 | 10 | [14] |
| EO switching | 26 | 137–418 | 260 | 1.898 | 0.1–0.5 | [15] |
| AO switching | 1136 | 40–270 | 110 | 2.796 | 10–50 | [16] |
| Co:MALO | 1000 | 8.5–30 | 1.3 | 140 | ~40–840 | [17] |
| Cavity dumping | 532 | 77.5–112 | **5320** | **47.5** | **0.1–5000** | This work |

[a]AO, acousto-optic; EO, electro-optic; MALO, MgAl$_2$O$_4$.

It is easy to see that the cavity-dumped pulsed laser has a significant advantage in laser performance.

The cavity-dumped pulsed laser has the highest pulse energy and peak power at 639 nm. Moreover, it also has the widest range of tunable repetition rates (0.1–5000 kHz), which can meet the needs of pulsed lasers with high repetition rates in some specific applications.

## 4. Conclusion

In summary, we confirm a high-performance cavity-dumped 639 nm all-solid-state pulsed laser based on a Pr:YLF crystal. At the repetition rate of 0.1 kHz, the maximum average output power, narrowest pulse width, highest pulse energy and highest peak power are 532 mW, 112 ns, 5.32 mJ and 47.5 kW, respectively, the fluctuation of average output power is 3.06% and the first-order diffracted beam quality factors $M^2$ are 2.18 (in the $x$ direction) and 2.04 (in the $y$ direction). An order-of-magnitude improvement in pulse energy and peak power of the 639 nm pulsed laser is achieved compared to the results of previous reports. In addition, the widest tunable range of repetition rates for the pulsed laser is obtained (0.1–5000 kHz). To the best of our knowledge, this is the first demonstration of a cavity-dumped solid-state pulsed laser in the visible band. This work provides an approach with great potential for obtaining high-performance pulsed lasers. In future work, we believe that the performance of the pulsed laser can be further improved by shortening the length of the resonant cavity and replacing the Pr:YLF crystal with a longer one. In addition, replacing the output of the first-order diffracted laser with a zeroth-order diffracted laser may also improve the performance of the laser.

## Acknowledgement

## References

1. R. G. Wheeland, Lasers. Surg. Med. **16**, 2 (1995).
2. M. E. Fermann and I. Hartl, Nat. Photonics **7**, 868 (2013).
3. O. Halabi and N. Chiba, Displays **30**, 97 (2009).
4. J. A. Creighton and D. G. Eadon, J. Chem. Soc. Faraday Trans. **87**, 3881 (1991).
5. Y. C. Chi, D. H. Hsieh, C. Y. Lin, H. Y. Chen, C. Y. Huang, J. H. He, B. Ooi, S. P. DenBaars, S. J. Nakamura, H. C. Kuo, and G. R. Lin, Sci. Rep. **5**, 18690 (2015).
6. P. W. Metz, F. Reichert, F. Moglia, S. Müller, D. T. Marzahl, C. Kränkel, and G. Huber, Opt. Lett. **39**, 3193 (2014).
7. F. Q. Li, J. Chen, and Y. P. Weng, AIP Adv. **13**, 085323 (2023).
8. Z. Cai, W. Yuan, R. Fang, X. Lin, and H. Xu, IEEE Photonics Technol. Lett. **36**, 393 (2024).
9. R. Fang, Z. P. Cai, and H. Y. Xu, Opt. Lett. **47**, 4267 (2022).
10. T. Gün, M. Philip, and H. Günter, Opt. Lett. **36**, 1002 (2011).
11. G. Huber, R. André, and H. Ernst, Proc. SPIE **6451**, 645102 (2007).
12. X. J. Lin, M. P. Chen, Q. C. Feng, S. H. Ji, S. W. Cui, Y. Zhu, B. Xiao, W. S. Li, H. Y. Xu, and Z. P. Cai, Opt. Laser. Technol. **142**, 107273 (2021).
13. J. Kojou, R. Abe, R. Kariyama, H. Tanaka, A. Sakurai, Y. Watanabe, and F. Kannari, Appl. Opt. **53**, 2030 (2014).
14. L. Jin, W. Dai, Y. Yu, Y. Dong, and G. Jin, Opt. Laser Technol. **129**, 106294 (2020).
15. Z. Yang, S. Z. Ud Din, P. Wang, C. Li, Z. Lin, J. Leng, J. Liu, L. Xu, Q. Yang, and X. Ren, Opt. Laser Technol. **148**, 107711 (2022).
16. Y. C. Xue, R. S. Zhang, Z. D. Dai, Z. Y. Wang, H. Y. Xu, and Z. P. Cai, Chin. Opt. Lett. **22**, 011402 (2024).
17. M. Badtke, H. Tanaka, L. J. Ollenburg, S. Kalusniak, and C. Kränkel, Appl. Phys. B **127**, 83 (2021).
18. B. Yao, H. Shi, T. Dai, Z. Shen, Y. Ju, G. Cai, and Y. Wang, Appl. Opt. **53**, 6816 (2014).
19. G. Cai, Y. Ju, B. Yao, W. Liu, X. Duan, and T. Dai, Opt. Express **22**, 9942 (2014).
20. T. Y. Dai, Z. G. Fan, H. W. Shi, Y. L. Ju, B. Q. Yao, Y. J. Jiang, and Y. Z. Wang, Optik **127**, 3175 (2016).
21. F. Cornacchia, A. Richter, E. Heumann, G. Huber, D. Parisi, and M. Tonelli, Opt. Express **15**, 992 (2007).
22. S. Khiari, M. Velazquez, R. Moncorge, J. L. Doualan, P. Camy, A. Ferrier, and M. Diaf, J. Alloys Compd. **451**, 128 (2008).
23. P. Wu, B. Xiao, Q. Feng, X. Lin, W. Li, H. Xu, and Z. Cai, J. Lumin. **235**, 118028 (2021).
24. W. Koechner, *Solid-State Laser Engineering* (Springer, 2013), Vol. **1**.
25. Y. Li, L. Jin, W. Dai, S. Li, Y. Dong, and G. Jin, Laser Phys. **30**, 125002 (2020).
26. Y. Jin, Y. Dong, L. Jin, H. Kang, and G. Jin, Opt. Laser. Technol. **166**, 109579 (2023).